RESEARCH ARTICLE

THE CHINESE JOURNAL OF
ARTIFICIAL INTELLIGENCE

A Differential Evolution Algorithm for Multi-objective Sparse Reconstruction

Xiaopei Zhu[1], Li Yan[1], Boyang Qu[1,*], Pengwei Wen[1] and Zhao Li[1]

[1]School of Electric and Information Engineering, Zhongyuan University of Technology, Zhengzhou, China

Abstract: *Aims*: This paper proposes a differential evolution algorithm to solve the multi-objective sparse reconstruction problem (DEMOSR).

Background: The traditional method is to introduce the regularization coefficient and solve this problem through a regularization framework. But in fact, the sparse reconstruction problem can be regarded as a multi-objective optimization problem about sparsity and measurement error (two contradictory objectives).

Objective: A differential evolution algorithm to solve multi-objective sparse reconstruction problem (DEMOSR) in sparse signal reconstruction and the practical application.

Methods: First of all, new individuals are generated through tournament selection mechanism and differential evolution. Secondly, the iterative half thresholding algorithm is used for local search to increase the sparsity of the solution. To increase the diversity of solutions, a polynomial mutation strategy is introduced.

Results: In sparse signal reconstruction, the performance of DEMOSR is better than MOEA/D-ihalf and StEMO. In addition, it can verify the effectiveness of DEMOSR in practical applications for sparse reconstruction of magnetic resonance images.

Conclusion: According to the experimental results of DEMOSR in sparse signal reconstruction and the practical application of reconstructing magnetic resonance images, it can be proved that DEMOSR is effective in sparse signal and image reconstruction.

Keywords: Multi-objective sparse reconstruction, differential evolution, compressed sensing, multi-objective optimization, iterative half thresholding algorithm, evolutionary algorithm.

1. INTRODUCTION

1.1. Single Objective Sparse Reconstruction

Compressed sensing (CS) [1] is an emerging information acquisition technology, which can reconstruct the original signal from a small number of measured values *via* the sparse characteristics of the signal. This theory has attracted great attention in the area of information theory, image processing, microwave imaging, pattern recognition, wireless communication and biomedical engineering [2-7]. With the emergence of Big data and the Internet of Things, the application value of the CS theory is increasingly prominent.

According to the CS theory, sparse reconstruction problems can be expressed as Eqs. (1) and (2):

$$\min_{x} \ \|x\|_0 \quad s.t. \quad y = Ax \tag{1}$$

$$\min_{x} \ \|x\|_0 \quad s.t. \quad \|y - Ax\|_2^2 \le \delta \tag{2}$$

where $x = (x_1, x_2, ..., x_n)^T$ is an n-dimensional sparse signal;

$y = (y_1, y_2, ..., y_m)^T$ is a m-dimensional measurement vector;

A is an $m \times n$ full-rank and over-complete sensing matrix with $m = n$; $\|x\|_0$, which is the zero-norm of x, it is used to represents the number of nonzero components of x, and also called the sparsity of the signal x. δ is a non-negative coefficient and represents the noise level.

It can be proven that these are NP-hard in (1) and (2) [8]. Greedy strategy is a common approach for reconstructing sparse signals. The well-known sparse reconstruction algorithms include basic pursuit algorithm [9], matching pursuit algorithm [10], and orthogonal matching pursuit algorithm [11]. However, these algorithms are difficult to find the global optimal solution, only an approximate solution can be provided as the final solution of the sparse reconstruction problem. In addition, the sparse reconstruction methods based on the regularization framework can also effectively recover the sparse signals. Sparse reconstruction problem can be formulated as L_q regularization problem (Eq. 3):

$$\min_{x} \ F(x) = \lambda \|x\|_q + \|y - Ax\|_2^2 \tag{3}$$

*Address correspondence to this author at the School of Electric and Information Engineering, Zhongyuan University of Technology, Zhengzhou, China; Tel: 0371-62506070; E-mail: quboyang@zut.edu.cn.

where λ is a non-negative coefficient; $\left\| y - Ax \right\|_2^2$ is a quadratic function for x; $\left\| x \right\|_q = \left(\sum_i x_i^q \right)^{\frac{1}{q}}, 0 \le q \le \infty$, it stands for the regularization term (L_q-norm of x). $q=0$, $q=1$ and $q=1/2$, which represent the regularization framework based on L_0, L_1, and $L_{1/2}$, respectively. Iterative hard thresholding method [12], iterative soft thresholding method [13], iterative half thresholding method [14] are the well-known solvers for L_0, L_1, and $L_{1/2}$. Sparsity estimation is often used in these methods, while the sparsity of the practical problems is often unknown. Moreover, the quality of the reconstructed solution is mainly affected by the setting of the regularization parameter λ in the regularization methods. In fact, a sparse reconstruction problem can be transformed into a multi-objective optimization problem and the two objectives are the sparsity and measurement error, which are in conflict with each other. This method avoids the influence of the regularization parameter on the reconstructed solution. The framework of the multi-objective optimization method is given in Eq. (4):

$$\min_x \ F(x)=(f_1(x), f_2(x)) \qquad (4)$$

where $f_1(x) = \left\| x \right\|_0$ is the sparsity of the sparse signal x; $f_2(x) = \left\| y - Ax \right\|_2^2$ is measurement error.

1.2. Multi-Objective Sparse Reconstruction

In recent years, some algorithms based on multi-objective frameworks, MOEA/D and NSGA-II, have been proposed for sparse reconstruction problems. In a study [15], a revised version of MOEA/D based on an iterative thresholding algorithm was proposed. The proposed algorithm is to find a part of the Pareto Front (PF) containing the knee solution, but it is not suitable for multi-objective sparse reconstruction problems with large noise levels. In order to find the optimal tradeoff solution, a multi-objective evolutionary algorithm based on NSGA-II was proposed and defined as StEMO [16]. In StEMO, a soft thresholding algorithm [17] was applied to increase the spread and the convergence rate. In addition, the performance of StEMO is significantly better than the traditional single-objective sparse reconstruction method, and it can recover sparse signals with noisy and noise-corrupted images. The key to a multi-objective sparse reconstruction problem is to quickly and accurately locate the PF near the knee solution. However, the purpose of StEMO is to approximate the entire PF, which consumes a lot of computational resources and ultimately reduces the convergence speed. Li *et al.* [18] presented a multi-phase multi-objective approach based on decomposition for sparse reconstruction (MOEA/D-L1/2), which optimizes subproblems by multi-phase search strategy. The multi-phase search strategy involves a chain manner in the first phase and a random manner in the second phase, the former aims at approximating the whole PF of the multi-objective sparse reconstruction problem. MOEA/D-L1/2 can effectively solve multi-objective sparse reconstruction problems with or without noise. In order to balance the exploration of the whole PF, the exploitation of the local PF with a k-sparse solution and reducing the computational complexi-

ty, a preference-based multi-objective evolutionary approach was proposed in another study [19]. Yan *et al.* designed a hybrid evolutionary algorithm with linear Bregman-based local search for multi-objective sparse reconstruction problems [20]. In order to accelerate convergence, the number of individuals and iterations in the linear Bregman-based local search is set to be adaptive. A multi-objective sparse reconstruction with transfer learning and localized regularization (MOSR-TLL) was proposed in a study [21]. MOSR-TLL used a knowledge transfer operator and localized regularization strategy to accelerate the convergence rate and improve the reconstruction accuracy. A multi-objective PSO with a one-dimension-dominated method was designed in another study [22], which can find a uniformly distributed PF and improve both the diversity and the convergence of the PF. Multi-objective evolutionary sparse recovery approach based on adaptive local search (ALSEMO) was proposed. Two local search methods are designed using the decomposition-based multi-objective evolutionary algorithm, and an adaptive local search mechanism is formed according to the competition strategy between the two methods in ALSEMO [23]. Most algorithms can solve multi-objective sparse reconstruction problems, and they cost a lot of time on the entire PF. They cannot provide fast reconstruction. However, the solution only close to the knee area is meaningful for the multi-objective sparse reconstruction problem.

Differential evolution (DE) was firstly proposed for continuous global optimization problems [24]. It is a heuristic random search model based on population, which is a branch of evolutionary algorithms. It has the advantages of dynamically tracking the current search situation, less control parameters, high convergence accuracy, strong robustness, and no need to rely on the feature information of the problem. Many multi-objective differential evolution (MODE) algorithms were proposed to solve MOPs. They have been successfully applied in the field of science and engineering [25-29]. They can generate a number of Pareto solutions in a single run; the reason is that most of them are based on population. Furthermore, existing algorithms still need to be improved in terms of convergence speed and reconstruction accuracy. In practical applications, signals or images with noise are also a challenge for multi-objective sparse reconstruction.

To our best knowledge, NSGA-II, MOEA/D and MOPSO, which are popular multi-objective frameworks, have been used for sparse reconstruction problems. MODE is a powerful population-based random search technique, which has the characteristics of simple structure and superior performance. The effectiveness of MODE has been proven in solving complex multi-objective optimization problem. However, it has not been used to solve sparse reconstruction problems. Therefore, this paper proposes a multi-objective differential evolution algorithm for sparse reconstruction problems.

2. METHODOLOGY

2.1. Proposed Algorithm

In order to solve sparse reconstruction problems, a multi-objective differential evolution algorithm is presented, and it introduced an iterative half thresholding algorithm as

a local search operator, which can improve the reconstruction accuracy.

2.1.1. Framework of the Proposed DEMOSR

The framework of the proposed DEMOSR is described in Fig. (**1**), with the corresponding pseudo-code given in Algorithm **1**. In Step 1, the initial population P^0, the observation matrix **A**, and the measurement vector **y** are randomly generated. The objective function values of individuals in the initial population are calculated according to formula (4). P^{Iters} is the population of the *Iters*-th generation. The iteration number is initialized as *Iters*=1 and the maximum number of the iterations is set to *maxIters*. In Step 2-Step 3, we use a tournament selection mechanism and differential evolution as mutation and crossover operators to generate a new individual. In order to increase the diversity of solutions, a polynomial mutation strategy is introduced in Step 4. The iterative half thresholding algorithm is introduced as a local search strategy to improve the sparsity of the solution (Step 5). Note that this strategy is used for each individual in the population, including newly generated individuals. In Step 6, the worst individual is removed from the current population P^{Iters}. In Step 7, we first sort the sparsity of individuals based on the non-dominant sorting strategy. Then, all non-dominated individuals are selected and the sparsity of the selected individual is updated. In Step 8, the method of the weighted sum of objective values is used to obtain the final solution [30].
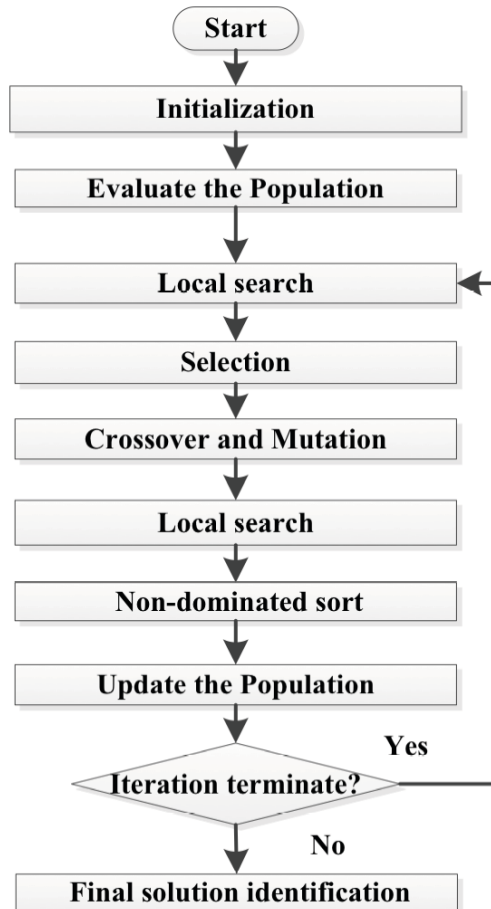

Fig. (1). The framework of DEMOSR.

Algorithm 1. The procedure of DEMOSR.

1 Input: The signal length, n; the number of observations m, the signal sparsity, k; the cross probability, Cr; the scaling factor, F; the population size, NP; the maximum number of iterations, *maxIters*; the maximum number of steps in local search *ls.*

2 Output: The optimal sparse solution.

3 Step 1: Initialization and evaluation

4 Step 1.1: Initialize the sensing matrix A and measurement vector y (Algorithm 2);

5 Step 1.2: Generate the initial population P^0 randomly;

6 Step 1.3: Evaluate the initial population P^0 according to formula (4);

7 Step 2: Selection

8 $temp1 = \text{BinaryTournamentSelection}(P^{Iters})$;

9 Step 3: Crossover

10 $temp2 = \text{DifferentialEvolutionCrossover}(temp1)$

11 Step 4: Mutation

12 $offspring = \text{PolynomialMutation}(temp2)$;

13 Step 5: Local search (Algorithm 3)

14 $offspring = \text{HalfThresholdSearch}(offspring, step)$;

15 Step 6: Updated population

16 $P^{Iters} = \text{Update}(P^{Iters}, offspring)$

17 Step 7: Select non-dominated individuals and update the sparsity;

18 Step 8: If the termination condition is satisfied

19 Terminate

20 Otherwise

21 Repeat Step 2-7, *Iters=Iters*+1;

22 End If

23 Step 9: Acquisition of the optimal solution: the method of weighted sum of objective values is used to acquire the final solution.

2.1.2. The Procedure of Initialization of the Sensing Matrix and Measurement Vector

The CS theory mainly consists of three parts: sparse representation, the design of the sensing matrix and sparse reconstruction. The focus of this paper is to design an effective algorithm for sparse reconstruction problems, and the other two parts are not studied in depth. In this subsection,

the procedure of initialization of the sensing matrix **A** and measurement vector **y** is presented in Algorithm **2**.

Algorithm 2. The procedure of initialization of the sensing matrix and measurement vector.

---

1 Input: n, m, k;

2 Output: the sensing matrix A and measurement vector y;

3 Step 1: Generate a signal $x_{\_opt}$ with all zero-dimensional elements;

4 Step 2: Randomly select k positions from the signal $x_{\_opt}$, and replace the element zeros at these k positions with randomly generated non-zero values, thereby converting the signal $x_{\_opt}$ into a sparse signal with sparsity degree k;

5 Step 3: Randomly generate an $m \times n$ observation matrix A and orthogonalize it;

6 Step 4: Obtain the observation vector $y \in R^{m \times 1}$ according to Eq. (1).

7 Step 5: Unitize the observation matrix A and measurement vector y. Then, output A and y.

2.1.3. Selection, Crossover and Mutation Operators

According to the binary tournament selection mechanism, we randomly select two individuals from the population P^{Iters} as parents. Then, the DE/rand/1 strategy is applied to generate a new individual which is described as follows (Eq. 5):

DE/rand/1:

$$X_i = x_{r1}^{Iters} + F \times \left(x_{r2}^{Iters} + x_{r3}^{Iters} \right) \tag{5}$$

where x_{r1}^{Iters} is the current individual in the *Iters* generation, x_{r2}^{Iters} and x_{r3}^{Iters} are randomly selected from the population of the *Iters* generation, which are different from each other; r_1, r_2, r_3 are randomly selected from the interval [1, NP], which are also different from each other.

The new individual is updated in the following way:

If rand<Cr

$$X_i^* = x_{r1}^{Iters} + F \times \left(x_{r2}^{Iters} + x_{r3}^{Iters} \right)$$

else

$$X_i^* = X_i$$

End

$$X_i^{*'} = \begin{cases} a_i, \text{with } X_i^* < a_i \\ X_i^*, \text{with } b_i \le X_i^* \le a_i, i = 1,2,L \ , NP \\ b_i, \text{with } b_i < X_i^* \end{cases}$$

where *rand* is a uniformly distributed random number in [0,1]; the scaling factor F=1; the crossover probability Cr=0.8; a_i, b_i are the minimum and maximum values of the i-th individual X_i.

In order to increase the diversity of the population, a polynomial mutation strategy [31] is introduced, which is widely used for multi-objective optimization. The polynomial mutation operator is described as follows:

If rand<p_m

$$X_i^{offspring} = X_i^{*'} + \delta_i \times \left(b_i - a_i \right)$$

else

$$X_i^{offspring} = X_i^{*'}$$

End

where p_m=1/n and η_m = 20 are the two control parameters for the mutation operator; r=random (0,1);

$$\delta_i = \begin{cases} \kappa - 1, r < 0.5 \\ 1 - \kappa, otherwise \end{cases}, \kappa = \left(2r + (1-2r) \times \left(\frac{b_i - X}{b_i - a_i} \right)^{\eta_m + 1} \right)^{\frac{1}{\eta_m + 1}}.$$

The iterative half thresholding algorithm is used to improve the new individual after the crossover operator and mutation operator. The iterative half thresholding algorithm is described in subsection 2.4. After executing the local search strategy, the new individual is merged with the current population, and then the individual with the worse ranks and crowding distances is eliminated *via* fast-elitist non-dominated sorting and crowding distance criteria [32]. Steps 2-7 are repeated until the termination condition is satisfied. In Step 9, a final solution is selected from the population by the weighted sum of objective values method.

2.1.4. Local Search Operator

The well-known sparse reconstruction methods based on regularization frameworks are iterative hard thresholding algorithm, iterative soft thresholding algorithm and iterative half thresholding algorithm. They are commonly used solvers for L_0, L_1, and $L_{1/2}$, respectively. Compared with other thresholding algorithms, the iterative half thresholding algorithm has a faster convergence speed and higher reconstruction accuracy [33]. In DEMOSR, we select the iterative half thresholding algorithm as a local search strategy. The main steps in the iterative half thresholding algorithm are gradient descent, regularization parameter optimization, and truncation operation. The procedure of the iterative half thresholding algorithm is presented in Algorithm **3**.

Algorithm 3. The procedure of iterative half thresholding algorithm.

---

1 Input: the sensing matrix and measurement vector y;

2 Output: x_{local}

3 Step 1: $t=0$, $c=\sqrt[3]{54}/4$, $x\_old= rand(n,1)$;

4 Step 2: Improve the solution x^t by gradient descent gradient descent $\tilde{x}=x^t + A^T\left(Ax^t - y\right)$;

5 Step 3: Take the absolute value of the elements in $\tilde{x}_i$, and sort them in descending order:

$$\left|\tilde{x}_{i_1}\right| \geq \left|\tilde{x}_{i_2}\right| \geq \cdots \left|\tilde{x}_{i_n}\right|$$

6 Step 4 Set regularization parameters λ_n;

7 Step 5: Threshold interruption, force the smaller absolute value in $\tilde{x}_i$ to zero:

If $\left|\tilde{x}_i\right| > c\lambda_n^{\frac{2}{3}}$

$$x_i^{t+1} = \psi_2(\tilde{x}_i)$$

otherwise

$$x_i^{t+1} = 0$$

End If

8 Step 6: If the termination condition is satisfied: $\left\|x^{t+1} - x^t\right\| < \varepsilon$ or $t \geq t_{\max}$

$x_{local} = x^{t+1}$, then terminate and output x_{local}

otherwise

$t=t+1$, then Repeat Step 2-Step 5

End If

where $\left|\tilde{x}_{i_1}\right|$ represents the largest element value among the absolute values of all elements in $\tilde{x}_i$, $\left|\tilde{x}_{i_n}\right|$ represents the smallest element value among the absolute values of all elements in $\tilde{x}_i$; $t_{\max}$ represents the maximum number of iterations; the regularization parameter λ_n is set to $\frac{\sqrt{96}}{9}\left|x_k^{t+1}\right|^{\frac{3}{2}}$; ε is an interruption threshold and is set to $\varepsilon =1E-10$. In Step 5, $\psi_2(\tilde{x}_i)$ can be formulated as (Eqs. 6 and 7):

$$\psi_2(\tilde{x}_i)=\frac{2}{3}\tilde{x}_i\left(1+\cos\left(\left(\frac{2\pi}{3}\right)-\left(\frac{2\phi(\tilde{x}_i)}{3}\right)\right)\right) \tag{6}$$

$$\phi(\tilde{x}_i)=\arccos\left(\frac{\lambda_n}{8}\left(\frac{\left|\tilde{x}_i\right|}{3}\right)^{-\frac{3}{2}}\right) \tag{7}$$

3. RESULTS AND DISCUSSION

3.1. Experimental Setting

In our experiments, we considered to recover sparse signals and reconstruct the magnetic resonance images. Nine artificial sparse instances without noise (P1-P9) are presented in Table **1**. n is the length of signal; m is the length of the observation vector, and k is the sparsity of the true signal. The dimensionality of these instances gradually increases, and the length of the corresponding observation vector gradually decreases. It also indicates that the difficulty of the artificial sparse instances increases gradually.

Considering that the smaller the ratio of m to k, the greater the difficulty of the test instances. The test instances are actually an ill-conditioned problem when the ratio m to k is less than 2. In this case, it is difficult to recover sparse solutions. As shown in Table **1**, the test instances P3, P6, and P9 are more difficult to solve than other instances of the same length. DEMOSR is coded by MATLAB and tested on the operating system Windows 10 Professional with 3.60GHz Intel (R) Core (TM) i7-7700 CPU 1170GB memory.

According to the literature [15-16,18], the experimental parameter settings corresponding to each algorithm in this paper are as follows:

MOEA/D-ihalf: step=10;

StEMO: the crossover rate is 0.5 and the mutation rate is 0.1;

DEMOSR: The probability of mating restriction is set to $\beta =0.9$; the scaling factor is $F=0.9$; the crossover probability is set to 1; the polynomial mutation operator is set to $p_m=1/n$ and $\eta_m = 20$.

For a fair comparison, each algorithm involved in this paper is executed 30 times independently. The parameters of the single-objective sparse reconstruction algorithm (BP, MP, OMP, IST) refer to the settings in the literature [9-11, 17]. The population number of three multi-objective algorithms (MOEA/D-ihalf, StEMO, DEMOSR) is all set to 100. The maximum number of the iterations is 5000. The observation matrix of all algorithms is a Gaussian random matrix, and the measured value vector is generated by $y=Ax$. The interruption condition of the algorithm is that the number of iterations is greater than or equal to the maximum number of iterations.

3.2. Experimental Results on Artificial Sparse Optimization Instances

In this section, in order to analyze and verify the effectiveness of DEMOSR, the experimental comparisons are made from the reconstruction error with different sparsity and the comparison with two multi-objective algorithms under the same conditions. An evaluation standard (Recon-

Table 1.   **The details of artificial sparse instances.**

Instance Name	Length of Signal n	Length of the Observation Vector m	True Sparsity k
P1	512	300	130
P2	512	280	130
P3	512	260	130
P4	1024	600	260
P5	1024	560	260
P6	1024	520	260
P7	5120	3000	1300
P8	5120	2800	1300
P9	5120	2600	1300

struction Error, *RE*) [20] is introduced, which is defined as follows:

$$RE = \frac{\left\| \boldsymbol{x}_{opt} - \boldsymbol{x}_{true} \right\|_2}{\left\| \boldsymbol{x}_{true} \right\|_2} \qquad (8)$$

where $\boldsymbol{x}_{opt}$ stands for the obtained optimal sparse signal; $\boldsymbol{x}_{true}$ represents the n-dimensional true signal.

For the same test instances, the sparsity is determined. When the length of the observation vector m is larger, the smaller the ratio of m to k (the sparsity of the test instance), the greater the difficulty of the test problem, and the true sparse solution or approximate sparse solution is easier to be found. Fig. (**2**) shows the impact of the length of the observation vector on *RE* in five sparse methods.
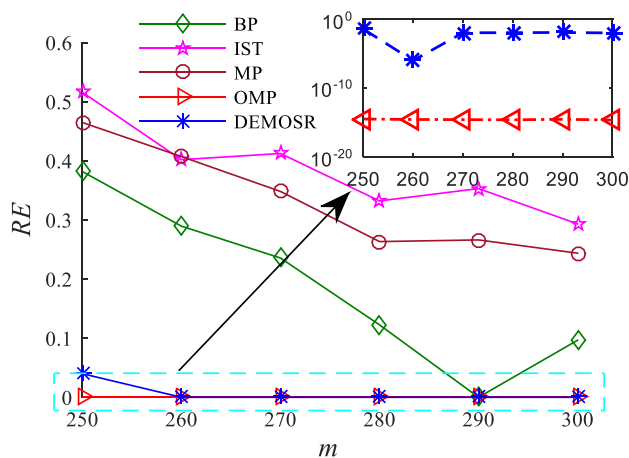

Fig. (2). Comparison of DEMOSR, BP, IST, MP and OMP with different lengths of the observation vector m on *RE*, where m=250, 260, 270, 280, 290, 300, respectively. (*A higher resolution / colour version of this figure is available in the electronic copy of the article*).

As shown in Fig. (**2**), as the length of the observation vector increases, the average value of *RE* corresponding to each algorithm shows a downward trend, except for OMP. The experimental result is consistent with the theoretical analysis. In addition, this also indirectly shows that the accuracy of the reconstructed solution *via* OMP and DEMOSR under different lengths of observation vector m is higher than that of other algorithms. However, an atom is selected to update the atom set in each iteration of the OMP, which will cause a huge cost of reconstruction time, especially for the long signals with noise. In addition, the number of iterations is closely related to the number of sparsity or measurement. With the increase of the number of iterations, time consumption will significantly increase. It has a slow speed for image signal reconstruction. In contrast, the diagonal nonlinearity of the threshold operator and the threshold of the function is that the iterative half thresholding algorithm can be applied to large-scale problems. Moreover, it is robust to observation noise. Therefore, we select the iterative half thresholding algorithm as a local search strategy in DEMOSR.

In the areas of sparse reconstruction, a solution has the same or approximate sparsity as the true sparse signal, and the measurement error corresponding to this solution is very small. It can be said that the algorithm successfully reconstructed the true sparse signal. In order to compare the performance of the proposed algorithm MOEA/D-ihalf and StEMO, the simulation experiments are conducted with nine artificial noiseless random sparse signals. The experimental results are shown in Fig. (**3**).

As shown in Fig. (**3**), the abscissa represents the sparsity of the test instances, and the ordinate represents the log of the measurement error of the reconstructed signal. It can be seen from (Fig. **3**) that the reconstruction solutions obtained by DEMOSR on seven artificial sparse instances (P1, P2, P3, P5, P6, P7 and P8) show a sharp drop near the true sparsity. The smallest measurement errors are all below 1E-10, some are even below 1E-20. For the same instance, MOEA/D-ihalf and DEMOSR have similar phenomena, while the measurement error of the former is larger. Compared with the other two algorithms, the measurement error of the obtained solution by StEMO is not competitive. Therefore, the performance of DEMOSR is better than the other two multi-objective sparse reconstruction algorithms.

To evaluate the performance of MOEA/D-iHalf, StEMO and DEMOSR, we give the statistical results (mean and standard deviation) of the measurement error and the sparsity in the experiments with different test instances. Tables **2** and **3** show the mean and standard deviation results of the reconstruction error and the sparsity with different test instances, respectively. The numbers given in bold show the results for the best-performing method in each row. Compared with the other two algorithms, the sparsity of the solution obtained by DEMOSR is closest to the sparsity of the true solution. In terms of the measurement error, the statistical results of the mean and standard deviation obtained by DEMOSR are smaller than MOEA/D-iHalf and StEMO. From the statistical results, we can see that StEMO has the largest measurement error on each test instance, indicating that the accuracy of the reconstructed signal is poor. This is consistent with the results observed in Fig. (**3**).

3.3. Practical Application

In the previous subsection, we compared and analyzed the performance of the proposed DEMOSR with MOEA/D-ihalf and StEMO by simulating nine artificial noiseless random sparse signals. It is worth noting that the research object of these simulation experiments is a set of one-dimensional sparse signals. In order to verify the efficacy of DEMOSR with a practical application and its ability to reconstruct two-dimensional sparse images, we considered to recover magnetic resonance images (SR1, SR2, SR3 and SR4) in this subsection. The magnetic resonance images are 128×128, but they are not sparse images. According to the basic idea of compressed sensing, an observation matrix, which is not related to the transform base, can project the magnetic resonance images into a low-dimensional space. Then, the original image can be reconstructed with high probability from these few projections. Based on this, Haar wavelets are used as sparse basis matrix to convert the magnetic resonance images into sparse images.

The original images, the reconstructed spatial images and the reconstructed images by DEMOSR are shown in Fig. (**4**), and the details of images and measurement errors of reconstructed images are shown in Table **4**. The simulation results show that DEMOSR can reconstruct the original

Table 2. **The statistical results (mean and standard deviation) of the sparsity of the solution obtained by MOEA/D-iHalf, StEMO and DEMOSR on nine instances.**

-	DEMOSR	MOEA/D-ihalf	StEMO
P1	**129.8 ± 0.70**	146.9 ± 15.35	108.6 ± 9.83
P2	**129.6 ± 0.52**	135.4 ± 21.92	113 ± 14.85
P3	**129.4 ± 0.84**	128.1 ± 7.00	113.1 ± 18.94
P4	**260 ± 0**	284.1 ± 35.77	202.89 ± 14.31
P5	**260 ± 0**	268.4 ± 43.85	203.2 ± 15.31
P6	**259.7 ± 0.67**	237.8 ± 38.50	193.1 ± 18.51
P7	**1304.1 ± 5.49**	1272 ± 134.68	1516.4 ± 363.98
P8	**1299.7 ± 9.94**	1049.4 ± 244.88	986.2 ± 115.41
P9	**1309.6 ± 14.10**	1095 ± 205.57	846.8 ± 96.16

Table 3. **The statistical results (mean and standard deviation) of the measurement error of the solution obtained by MOEA/D-iHalf, StEMO and DEMOSR on nine instances.**

| -	DEMOSR	MOEA/D-ihalf	StEMO
P1	**3.93E-06 ± 1.17E-05**	1.88E-05 ± 4.61E-05	19.40 ± 5.39
P2	**7.52E-06 ± 1.54E-05**	1.37E-01 ± 2.61E-01	24.18 ± 7.55
P3	**1.40E-02 ± 4.41E-02**	1.11E-01 ± 1.97E-01	24.83 ± 8.66
P4	**9.35E-07 ± 2.95E-06**	2.45E-03 ± 7.40E-03	44.29 ± 10.40
P5	**3.34E-15 ± 1.06E-14**	3.32E-01 ± 9.70E-01	59.33 ± 18.04
P6	**6.98E-11 ± 2.06E-10**	8.84E-01 ± 9.43E-01	75.10 ± 14.72
P7	**2.87E-05 ± 8.86E-05**	8.30E-01 ± 1.38	8.61E-01 ± 1.60
P8	**1.10E-04 ± 3.48E-04**	4.50 ± 3.58	298.95 ± 84.27
P9	**1.49E-02 ± 3.53E-02**	2.8962 ± 3.7052	462.54 ± 96.30
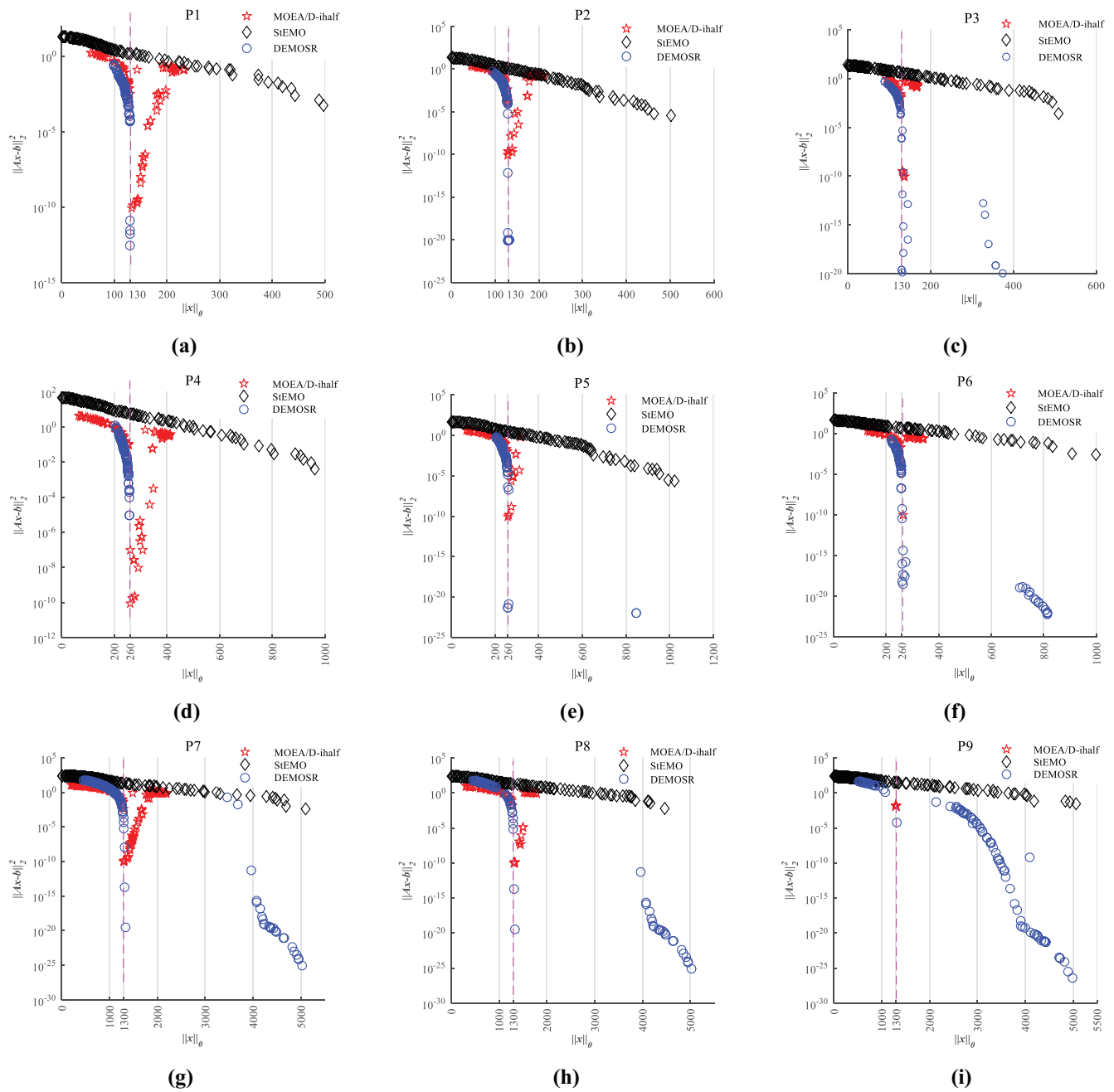
Fig. (3). Performance of DEMOSR, MOEA/D-ihalf and StEMO on nine artificial sparse instances without noise (P1-P9 correspond to (**a-i**). (*A higher resolution / colour version of this figure is available in the electronic copy of the article*).
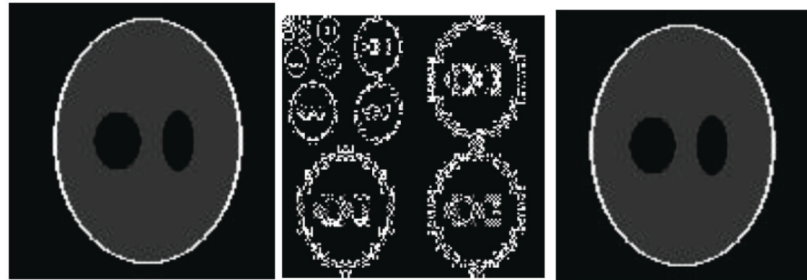

(a) SR1: The original image the reconstructed spatial image the reconstructed image
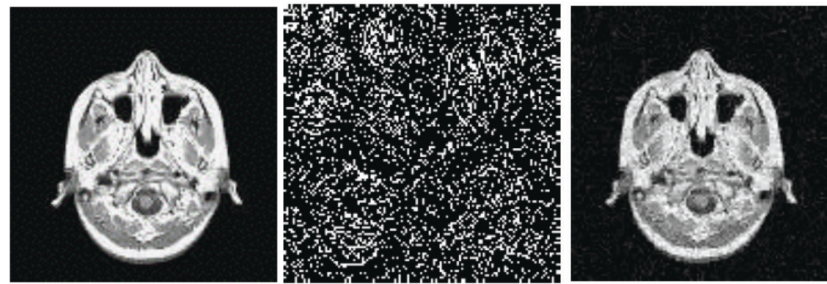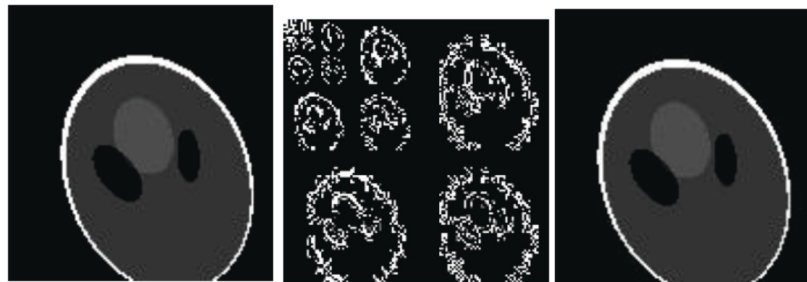
(b) SR2: The original image the reconstructed spatial image the reconstructed image

(c) SR3: The original image the reconstructed spatial image the reconstructed image

(d) SR4: The original image the reconstructed spatial image the reconstructed image

Fig. (4). The original images, the reconstructed spatial images and the reconstructed images by DEMOSR.

Table 4.   The details of images and measurement errors of reconstructed images.

Magnetic Resonance Images	Sparsity	Transformed Sparsity	Measurement Error
SR1	16266	7473	2.40E+03
SR2	16247	7147	2.45E+03
SR3	8020	4524	6.37E-05
SR4	7806	4566	1.66E-05

image. Compared with the original image, the reconstructed image is clearer. The reconstructed images of SR1 and SR2 contain noise, while the reconstructed images of SR3 and SR4 are more effective and accurate. As shown in Table **4**, the measurement errors of SR1 and SR2 are also larger than that of SR3 and SR4. This also further verified the effectiveness of DEMOSR in the image reconstruction, while it is not suitable for the reconstructed magnetic resonance images with noise.

CONCLUSION

In this paper, we propose a differential evolution algorithm for solving multi-objective sparse reconstruction prob-

lems (DEMOSR), which involves four strategies: tournament selection mechanism, DE operator, polynomial mutation strategy and iterative half-threshold algorithm. The experimental results on nine artificial sparse instances without noise show that the performance of the proposed method is better than MOEA/D-ihalf and StEMO, which are commonly used for sparse reconstruction. It also can be proved that DEMOSR maintains a high exploration ability and convergence rate. Practical applications also prove the effectiveness of DEMOSR in sparse image reconstruction.

For future work, we will conduct more research on improving the ability of DEMOSR to solve sparse reconstruc-

tion problems, increasing the robustness of DEMOSR, and reducing the computational complexity of DEMOSR.

CONSENT FOR PUBLICATION

Not applicable.

AVAILABILITY OF DATA AND MATERIALS

All data generated or analysed during this study are included in this published article.

FUNDING

CONFLICT OF INTEREST

The authors declare no conflict of interest, financial or otherwise.

ACKNOWLEDGEMENTS

REFERENCES

[1]   Donoho, D.L. Compressed sensing. *IEEE Trans. Inf. Theory,* **2006**, *52*(4), 1289-1306.
http ://dx.doi.org/10.1109/TIT.2006.871582

[2]   Stanković, L.; Sejdić, E.; Stanković, S.; Daković, M.; Orović, I. A tutorial on sparse signal reconstruction and its applications in signal processing. *Circuits Syst. Signal Process.,* **2019**, 38, 1206-1263.

[3]   Lai, Z.; Mo, D.; Wen, J.; Shen, L.; Wong, W.K. Generalized robust regression for jointly sparse subspace learning. *IEEE Trans. Circ. Syst. Video Tech.,* **2019**, *29*(3), 756-772.
http ://dx.doi.org/10.1109/TCSVT.2018.2812802

[4]   Seo, J.W.; Kim, S.D. Dynamic background subtraction *via* sparse representation of dynamic textures in a low-dimensional subspace. *Signal Image Video Process.,* **2016**, *10*(1), 29-36.
http ://dx.doi.org/10.1007/s11760-014-0697-5

[5]   Shah, P.; Moghaddam, M. A fast level set method for multimaterial recovery in microwave imaging. *IEEE Trans. Antenn. Propag.,* **2018**, *66*(6), 3017-3026.

[6]   Irmak, E.; Ertas, A.H. A review of robust image enhancement algorithms and their applications.*In 2016 IEEE Smart Energy Grid Engineering (SEGE)*; IEEE, **2016**, pp. 371-375.
http ://dx.doi.org/10.1109/SEGE.2016.7589554

[7]   Irmak, E.; Erçelebi, E.; Ertaş, A.H. Brain tumor detection using monomodal intensity based medical image registration and MATLAB. *Turk. J. Electr. Eng. Comput. Sci.,* **2016**, *4*(24), 2730-2746.
http ://dx.doi.org/10.3906/elk-1403-75

[8]   Davis, G. Adaptive nonlinear approximations, Ph.D. dissertation, New York University, Graduate School of Arts and Science: New York, NY, USA, **1994**.

[9]   Chen, S.S.; Donoho, D.L.; Saunders, M.A. Atomic decomposition by basis pursuit. *SIAM Rev.,* **2001**, *43*(1), 129-159.
http ://dx.doi.org/10.1137/S003614450037906X

[10]   Mallat, S.G.; Zhang, Z. Matching pursuits with time-frequency dictionaries. *IEEE Trans. Signal Process.,* **1993**, *41*(12), 3397-3415.
http ://dx.doi.org/10.1109/78.258082

[11]   Pati, Y.C.; Rezaiifar, R.; Krishnaprasad, P.S. Orthogonal matching pursuit: Recursive function approximation with applications to wavelet decomposition *Proceedings of 27th Asilomar conference on signals, systems and computers,* **1993**, pp. 40-44.
http ://dx.doi.org/10.1109/ACSSC.1993.342465

[12]   Blumensath, T. Accelerated iterative hard thresholding. *Signal Processing,* **2012**, *92*(3), 752-756.
http ://dx.doi.org/10.1016/j.sigpro.2011.09.017

[13]   Hyberts, S.G.; Milbradt, A.G.; Wagner, A.B.; Arthanari, H.; Wagner, G. Application of iterative soft thresholding for fast reconstruction of NMR data non-uniformly sampled with multidimensional Poisson Gap scheduling. *J. Biomol. NMR,* **2012**, *52*(4), 315-327.
http ://dx.doi.org/10.1007/s10858-012-9611-z PMID: 22331404

[14]   Xu, Z.; Chang, X.; Xu, F.; Zhang, H. L1/2 regularization: A thresholding representation theory and a fast solver. *IEEE Trans. Neural Netw. Learn. Syst.,* **2012**, *23*(7), 1013-1027.
http ://dx.doi.org/10.1109/TNNLS.2012.2197412 PMID: 24807129

[15]   Li, H.; Su, X.; Xu, Z.; Zhang, Q. MOEA/D with iterative thresholding algorithm for sparse optimization problems *International Conference on Parallel Problem Solving from Nature,* **2012**, pp. 93-101.
http ://dx.doi.org/10.1007/978-3-642-32964-7_10

[16]   Li, L.; Yao, X.; Stolkin, R.; Gong, M.G.; He, S. An evolutionary multi-objective approach to sparse reconstruction. *IEEE Trans. Evol. Comput.,* **2014**, *18*(6), 827-845.
http ://dx.doi.org/10.1109/TEVC.2013.2287153

[17]   Herrity, K.K.; Gilbert, A.C.; Tropp, J.A. Sparse approximation *via* iterative thresholding *IEEE International Conference on Acoustics Speech and Signal Processing Proceedings,* **2006**, *vol. 3*, pp. III-III.

[18]   Li, H.; Fan, Y.; Zhang, Q.; Xu, Z.; Deng, J. A multi-phase multi-objective approach based on decomposition for sparse reconstruction *Proc. IEEE Congress on Evolutionary Computation,* **2016**, pp. 601-608.

[19]   Li, H.; Zhang, Q.; Deng, J.; Xu, Z-B. A preference-based multi-objective evolutionary approach for sparse optimization. *IEEE Trans. Neural Netw. Learn. Syst.,* **2018**, *29*(5), 1716-1731.
http ://dx.doi.org/10.1109/TNNLS.2017.2677973 PMID: 28368832

[20]   Yan, B.; Zhao, Q.; Wang, Z.; Zhao, X.Y. A hybrid evolutionary algorithm for multi-objective sparse reconstruction. *Signal Image Video Process.,* **2017**, *11*(6), 993-1000.
http ://dx.doi.org/10.1007/s11760-016-1049-4

[21]   Yan, B.; Zhao, Q.; Zhang, J.A.; Wang, Z. Multi-objective sparse reconstruction with transfer learning and localized regularization. *IEEE Access,* **2020**, *8*, 184920-184933.
http ://dx.doi.org/10.1109/ACCESS.2020.3029968

[22]   Yue, C.T.; Liang, J.; Qu, B.Y.; Han, Y.H.; Zhu, Y.S.; Crisalle, O.D. A novel multiobjective optimization algorithm for sparse signal reconstruction. *Signal Processing,* **2020**, *167*, 107292
http ://dx.doi.org/10.1016/j.sigpro.2019.107292

[23]   Liu, H.L.; Chi, J.L.; Deng, Q.Y.; Peng, X.; Pei, T.R. Multi-Objective Evolutionary Sparse Recovery Approach Based on Adaptive Local Search. *J. Compu. Res. Develop.,* **2019**, *56*(7), 1420.

[24]   Das, S.; Suganthan, P.N. Differential evolution: A survey of the state-of-the-art. *IEEE Trans. Evol. Comput.,* **2010**, *15*(1), 4-31.
http ://dx.doi.org/10.1109/TEVC.2010.2059031

[25]   Babu, B.V.; Anbarasu, B. Multi-objective differential evolution (MODE): An evolutionary for multi-objective optimization problems. (MOOPs *Proceedings of the Third International Conference on Computational Intelligence, Robotics, and Autonomous Systems (CIRAS-2005),* Singapore, 2005.

[26]   Ali, M.; Siarry, P.; Pant, M. An efficient differential evolution-based algorithm for solving multi-objective optimization problems. *Eur. J. Oper. Res.,* **2012**, *217*(2), 404-416.

[27]   Fan, R.; Wei, L.; Li, X.; Zhang, J.; Fan, Z. Self-adaptive weight vector adjustment strategy for decomposition-based multi-objective differential evolution algorithm. *Soft Comput.,* **2020**, *24*(17), 13179-13195.
http ://dx.doi.org/10.1007/s00500-020-04732-y

[28]   Ren, W.; Wang, Y.; Han, M. Time series prediction based on echo state network tuned by divided adaptive multi-objective differential evolution algorithm. *Soft Comput.,* **2021**, *25*(6), 4489-4502.
http ://dx.doi.org/10.1007/s00500-020-05457-8

[29]   Qiao, B.; Liu, J.; Hao, X. A multi-objective differential evolution algorithm and a constraint handling mechanism based on variables proportion for dynamic economic emission dispatch problems. *Appl. Soft Comput.,* **2021**, *108*, 107419.

http ://dx.doi.org/10.1016/j.asoc.2021.107419

[30]   Liang, J.J.; Zhu, X.P.; Yue, C.T.; Li, Z.H.; Qu, B.Y. Performance analysis on knee point selection methods for multi-objective sparse optimization problems. *IEEE Congress on Evolutionary Computation (CEC),* **2018**, pp. 1-8.
http ://dx.doi.org/10.1109/CEC.2018.8477915

[31]   Zille, H.; Ishibuchi, H.; Mostaghim, S.; Nojima, Y. Mutation operators based on variable grouping for multi-objective large-scale optimization *IEEE Symposium Series on Computational Intelligence,* **2016**, pp. 1-8.

http ://dx.doi.org/10.1109/SSCI.2016.7850214

[32]   Deb, K.; Pratap, A.; Agarwal, S.; Meyarivan, T. A fast and elitist multi-objective genetic algorithm: NSGA-II. *IEEE Trans. Evol. Comput.,* **2002**, *6*(2), 182-197.
http ://dx.doi.org/10.1109/4235.996017

[33]   Liu, C.; Liang, Y.; Luan, X.Z.; Leung, K.S.; Chan, T.M.; Xu, Z.B.; Zhang, H. The *L*1/2 regularization method for variable selection in the Cox model. *Appl. Soft Comput.,* **2014**, *14*, 498-503.
http ://dx.doi.org/10.1016/j.asoc.2013.09.006